J. Eng. Technol. Sci., Vol. 51, No. 5, 2019, 707-728

Drought Event Analysis and Projection of Future Precipitation Scenario in Abaya Chamo Sub-Basin, Ethiopia

Ayele Elias Gebeyehu[1], Zhao Chunju[1*], Zhou Yihong[1] & Negash Wagasho[2]

[1]Department of Hydraulic Engineering, College of Hydraulic and Environmental Engineering, China Three Gorges University, Yichang443003, China
[2]Ethiopian Ministry of Water, Irrigation and Electricity, Addis Ababa, Ethiopia
*E-mail: chunju.zhao@ctgu.edu.cn

Abstract. Monthly observed and future precipitation magnitudes were subjected to statistical trend analysis to examine possible time series behavior. Future precipitation was downscaled from large-scale output through statistical downscaling. The observed and downscaled future precipitation was analyzed for drought events using the Standardized Precipitation Index (SPI) method. In the Abaya Chamo sub-basin, Ethiopia precipitation is explained by below average magnitudes in most of the low land area, characterized by moderate to extreme drought episodes. Nine drought events were discerned during the period of 1988 to 2015, i.e. once in three years, resulting in harvest failure and subsequent food insecurity. The NCEP-NCAR and CanESM2 model predictors were used to statistically downscale the precipitation data. The monthly observed and downscaled precipitation magnitudes were in good agreement. The RCP-2.6, RCP-4.5 and RCP-8.5 long-term future scenarios were computed to evaluate future drought patterns. The mean annual precipitation scenario decreased by 0.2% to 13.7%, 0.5% to 6.4% and 0.1% to 1.3% for the period from 2016 to 2040, 2050s and 2080s respectively. The increase in mean precipitation was projected to be 0.7% to 12.2%, 0.2% to 11.7% and 0.1% to 17.8% for the period from 2016 to 2040, 2050s and 2080s respectively. The present analysis may provide useful information associated to drought events to decision makers and can be used as a basis for future research in this area.

Keywords: *Abaya Chamo sub-basin; drought event; precipitation scenario; SDSM; SPI.*

1 Introduction

Fresh water demand around the world is affected by higher living standards, population growth, agricultural and industrial activities growth, LULC changes, climate change, degradation in water quality and soil, and numerous other factors. The significant spatial and temporal inconsistency of water resources frequently results in water shortages in different areas and in different seasons or time periods. This issue becomes far more pressing during periods of

Received October 24th, 2018, 1st Revision May 8th, 2019, 2nd Revision August 2nd, 2019, Accepted for publication September 20th, 2019.
 ISSN: 2337-5779, DOI: 10.5614/j.eng.technol.sci.2019.51.5.8

drought. Drought is a natural and periodic climate feature that occurs in almost all climatic regimes [1]. The main reason for drought is insufficient precipitation and, in particular, the distribution, intensity, and timing of this insufficiency in relation to the existing water demand, storage, and use. Thus, drought is an extended period of water shortage that naturally occurs when an area obtains precipitation below normal amounts for several months or seasons [2].

Meteorological drought comprises of temporary below average rainfall and results in decreased water resource accessibility and carrying ability of ecosystems [3], which influences the environment, human lives and economic activities [4]. In recent years, several researchers have investigated drought events in different areas of the world [5-12] despite the fact that drought phenomena are challenging to identify and monitor because of their complex nature. Commonly, drought severity is assessed using drought indices [13]. Among the available methods, the Standardized Precipitation Index (SPI) has found extensive application worldwide because it can be assessed for various timescales and permits the investigation of different drought classifications [14]. Because of this, the SPI method is considered a standout among the most powerful and effective drought indices [15]. Additionally, the assessment of the SPI only requires rainfall data, making it simpler to compute than more complex indices, and permits the evaluation of drought circumstances in various regions and for various time periods [11,14,16-18].

Rainfall in Ethiopia is influenced by the wider El Niño-Southern Oscillation (ENSO) effects and local weather patterns [19]. The central and east-central Pacific Ocean weather system also triggers dominant weather variables such as temperature and air pressure above the ocean surface. This impacts the air pressure above the ocean and the pattern of wind and rainfall crosswise over an extensive area of the tropics and sub-tropics [20]. Rainfall distribution in Ethiopia is also manifested by altitudinal variability and seasonality. Some geographical territories of the country receive high annual rainfall (exceeding 1500 mm). However, in the arid and semi-arid regions of the country, very low rainfall for limited periods is observed. Based on topographic altitude, the country is divided into three climatic zones, namely 'Dega' (Cool Zone with altitude above 2400 m), 'Woina Dega' (Subtropical Zone) and 'Kolla' (Tropical Zone with altitude below 1500 m) [20,21].

The annual seasons resulting from Earth's orbit around the Sun and its axial tilt relative to the ecliptic plane [19] are noticeable in Ethiopia. The Kiremt season is a heavy rain season in all parts of Ethiopia except the southeastern and southern parts, which receive significant amounts of rainfall from June to August. The Belg season is a light rainy season commonly observed in the southeastern and southern parts of Ethiopia from September to November. The Bega season (December to February) is a dry season in all parts of the country. The Tseday season is a rainfall season in the southeastern and southern parts from March to May and imparts the maximum annual solar radiation all over the country [22].

The national economy and food security are highly dependent on rain-fed agriculture [21,23,24]. Frequent droughts as a result of rainfall variability and global climate change have hampered agricultural productivity because of water shortages and related impacts. The recent historical records indicate that the frequency of drought occurrence falls below once in five years [25]. In a period of drought, the amount of total rainfall is below average, resulting in low food crop production, which affects millions of the human and animal population [21,24-28]. The major drought episodes of 1965-66, 1972-73, 1983-84, 1987-88, 1991-92, 1997, 1999-2000, 2002, 2009 and 2015-16, caused by absence or delay in spring (Tseday) and summer (Kiremt) rains, had negative social and economic ramifications [24-26,29]. In Ethiopia, El Niño episodes have a high probability to cause rainfall above or below normal. The drought events of 1987-88, 1991-92, 2002, 2009 and 2015-16 were associated with El Niño episodes [30].

The summer (Kiremt) and annual rainfall trends in southern, eastern and southern Ethiopia have declined since 1982 [21]. In the Abaya Chamo sub-basin, the climate varies from tropical to alpine and the rainfall pattern is bimodal. The main rainy season in the catchment is from March to May and the second rainy season is from September to October. However, in the northern part of the sub-basin, substantial amounts of rainfall are observed between July and October [31]. The sub-basin’s agricultural productivity is highly dominated by rain-fed crops and traditional farming methods and hence highly influenced by rainfall variability. Thus, it is vital to assess the future rainfall variability and recommend possible adaptation and mitigation methods. This study was aimed at evaluating the historical rainfall variability using the MK trend test method, analyzing drought characteristics using the Standardized Precipitation Index (SPI), and forecasting the future rainfall scenario using Statistical Downscaling Model (SDSM) in the Abaya Chamo sub-basin.

2 Material and Methods

2.1 Study Area

The Abaya Chamo sub-basin is part of the Ethiopian rift valley basin located in the South Nations, Nationalities and Peoples’ Region (SNNPR). It is located at 5°51.5’N to 8°8’N latitude and 37°16.3’E to 38°39.3’E longitude [32] and the altitude varies from 4200 m.a.s.l to 1108 m.a.s.l [31]. In the sub-basin, the mean annual total precipitation varies from 400 mm to 2,300 mm. Lake Abaya and Lake Chamo are two endorheic lakes situated in the sub-basin created by volcanic activity during the Pliocene and Holocene [31]. Observed meteorological data from fourteen stations in the sub-basin were used for further analysis. Figure 1 shows the location of the study area.

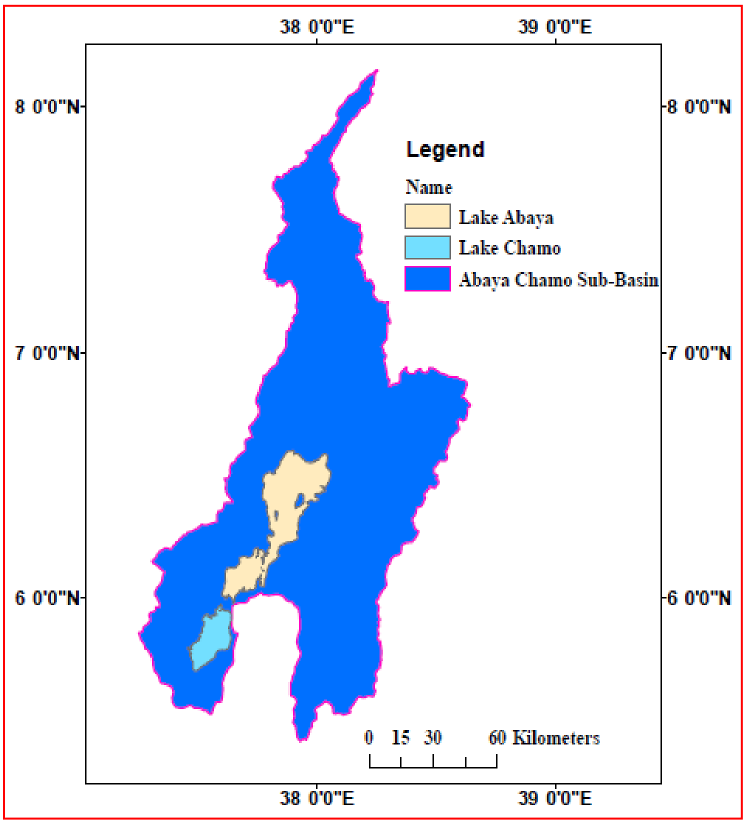

Figure 1 Location of Abaya Chamo Sub-Basin.

2.2 Data Used

Daily rainfall data records for fourteen meteorological stations in Abaya Chamo sub-basin were acquired from the Ethiopian National Meteorological Agency. The second generation Canadian Earth System Model (CanESM2) developed by the Canadian Centre for Climate Modeling and Analysis (CCCma) of Environment Canada for SDSM input were accessed from online sources [33]. The CanESM2 output has three different representative concentration pathway (RCP) scenarios, i.e. RCP-2.6, RCP-4.5 and RCP-8.5. The daily rainfall records for this study covered the period from 1988 to 2015. The arithmetic mean and the normal ratio methods were used to fill in the missing rainfall records. The observed rainfall data were further checked for consistency using the double mass curve (DMC) method.

2.3 Methods

2.3.1 Consistency and Trend Analysis

The observed rainfall records were checked for consistency and possible systematic anomalies because of man-induced changes or failure of the recording devices to measure actual values within the catchment area throughout the record period. Inconsistencies may occur due to rain gage station moving to another location, obstruction by tall buildings around the station, ecosystem changes and observation errors. Within the plot of cumulated precipitation of each station against the cumulated precipitation of the group of base stations, a break in the slope indicates inconsistency of the records, which can be corrected with the following formulation [34,35].

$$P_{cx} = P_x \frac{S_c}{S_o} \tag{1}$$

where:

P_{cx} – corrected precipitation record
P_x – original precipitation record
S_c – corrected slope of DMC
S_o – original slope of DMC

The most common non-parametric tests for working with time series trends are the Mann-Kendall (MK) and Spearman's rho tests [36]. The MK trend test is not affected by missing data and the length of the time series. Therefore, in this study, the Mann-Kendall non-parametric method was used to analyze for possible trends in the rainfall observed at fourteen meteorological stations in the sub-basin.

The MK trend analysis method is a commonly applied approach for meteorological and hydrological trend analysis [37-46]. The test was computed for n time series values (x_1, x_2, x_3, …, x_n) as follows [47]:

$$S = \sum_{i=1}^{n-1}\left[\sum_{j=i+1}^{n} \operatorname{sgn}\left(x_i - x_j\right)\right] \tag{2}$$

where

$$\operatorname{sgn}\left(x_i - x_j\right) = \begin{cases} 1 \rightarrow for, x_i - x_j > 0 \\ 0 \rightarrow for, x_i - x_j = 0 \\ -1 \rightarrow for, x_i - x_j < 0 \end{cases} \tag{3}$$

xi and xj are annual values, I > j and n is the number of data points.

If the null hypothesis (Ho) is true, then S is approximately distributed with:

$$E\left(S\right) = 0 \tag{4}$$

$$Var(S) = \frac{n\left(n-1\right)\left(2n+5\right)}{18} \tag{5}$$

The variance of standard deviation is corrected for tied elements when n ≥ 10 as:

$$Var(S) = \frac{n\left(n-1\right)\left(2n+5\right) - \sum_{i+1}^{m} t_i\left(i-1\right)\left(2i+5\right)}{18} \tag{6}$$

$$Z = \begin{cases} \dfrac{S-1}{\sqrt{Var(S)}} \rightarrow if, S > 0 \\ 0 \rightarrow if, S = 0 \\ \dfrac{S+1}{\sqrt{Var(S)}} \rightarrow if, S < 0 \end{cases} \tag{7}$$

where *E(S)* is the expected value, *Var(S)* is the variance of standard deviation, *m* is the number of tied elements, t_i is the number of tied data points of extent *i*, and *Z* is the standard normal deviate. If -1.96 < Z < 1.96, the null hypothesis is significant at 95% confidence level [48]. (H_o) of that the factors are identically and independently distributed is rejected if /Z/ > $Z_{1-\alpha/2}$ at α level of significance [39,47].

2.3.2 Standardized Precipitation Index (SPI)

Drought occurs after absence or shortage of rainfall. To determine drought indices several methods have been used in the literature, such as the Aggregate Drought Index (ADI) [49], Drought Severity Index (DSI) [50], Palmer Drought Index (PDI) [51], Regional Deficiency Index (RDI) [52], Regional Drought Area Index (RDAI) [53], Standardized Hydrological Index (SHI) [54], Standardized Precipitation Index (SPI) [55], Standardized Runoff Index (SRI) [56] and Stream flow Drought Index (SDI) [57, 58].

In the present study, the historical drought over the sub-basin was assessed by the Standardized Precipitation Index approach. To compute the time series of the SPI, the model developed by the National Drought Mitigation Center, University of Nebraska-Lincoln was used.

Standardized precipitation is basically the distinction of precipitation from the average for a predefined period divided by the standard deviation, where the average and standard deviation are resolved from past records [55]. The input parameter for SPI is monthly rainfall data. SPI is a simple and powerful drought index and can be computed for time scales of 1, 3, 6, 12, 24, and 48 months [55,59,60]. For each meteorological station in the Abaya Chamo sub-basin SPI was computed for time scales of 3 and 12 months.

The first procedure in the computation of the SPI is determining the probability density function of long-term observed and simulated rainfall data. When this has been resolved, the aggregate probability of observed and simulated rainfall amount is processed. Then a Gaussian function is used to calculate the probability [25,61].

Table 1 shows the classification in SPI to classify the drought intensity results [55]. If the rainfall magnitude is above average, the SPI value is positive and the value indicates wet events. However, if the rainfall magnitude is below average, the SPI value is negative and is associated with drought events [55,62].

Table 1 SPI event classification [55].

SPI	Event
≥ 2.0	Extremely wet
[1.5,2.0)	Very wet
[1.0, 1.5)	Moderately wet
(-1.0, 1)	Near normal
(-1.5, -1.0]	Moderately dry
(-2.0, -1.5]	Severely dry
≤ -2.0	Extremely dry

2.3.3 Statistical Down Scaling Model (SDSM)

SDSM, developed by [63], is one of the most reliable tools for studying future climate change scenarios. The input parameters for SDSM are: daily observed rainfall or temperature as predictands and GCM predictor data sets. SDSM is calibrated and validated using NCEP-NCAR outputs and daily observed climate data. To generate a future scenario, downscaled, calibrated and validated climate outputs and NCEP-NCAR outputs are used.

The output from the CanESM2 scenario can be used to forecast a future scenario [64]. The predictors downloaded from Canadian Center for Climate Modeling and Analysis with spatial resolution of 2.8125° latitude and 2.8125° longitude were used. Calibration and validation output results of SDSM were checked by using coefficient of determination (R^2), Nash-Sutcliffe efficiency (NSE) and percent bias (PBIAS) to assess the performance of the model. Figure 2 shows the overall technical process of statistical downscaling of the model to generate the future precipitation scenario. The R^2, NSE and PBIAS are calculated as follows:

$$R^2 = \left[\frac{\sum_{i=1}^{n} (O_i - O_{ave})(S_i - S_{ave})}{\sqrt{\sum_{i=1}^{n} (O_i - O_{ave})^2} \sqrt{\sum_{i=1}^{n} (S_i - S_{ave})^2}} \right] \tag{8}$$

$$NSE = 1 - \frac{\sum_{i=1}^{n} (O_i - S_i)^2}{\sum_{i=1}^{n} (O_i - O_{ave})^2} \tag{9}$$

$$PBIAS = \left[\frac{\sum_{i=1}^{n} (O_i - S_i)}{\sum_{i=1}^{n} O_i} \right] * 100 \tag{10}$$

where O_i and S_i- are the observed and simulated data series, respectively; O_{ave} and S_{ave}- are the mean values of the observed and simulated data series, respectively; and *n*- is the length of the time series.

In SDSM, screening of reasonable predictors for downscaling predictands is one of the most essential steps [65,66]. The fundamental reason for screen variable operation is to help the user in the decision of fitting the downscaling predictor variables [63]. The selection of predictors can be different for various geographical regions based on the properties of the predictor and the predictand to be downscaled [66,67]. Reasonable predictors are selected by three methods in SDSM, such as analysis (percentage of variance), correlation matrix and scatter plot. In this study, analysis and a correlation matrix were used to select suitable predictors. The selected appropriate predictor variables for all stations were: mean sea level pressure, 1000 hPa wind speed, 1000 hPa zonal wind component, 1000 hPa meridional wind component, 1000 hPa wind direction, 1000 hPa divergence of true wind, 500 hPa Geopotential, 850 hPa Geopotential, 1000 hPa specific humidity and air temperature at 2 m.

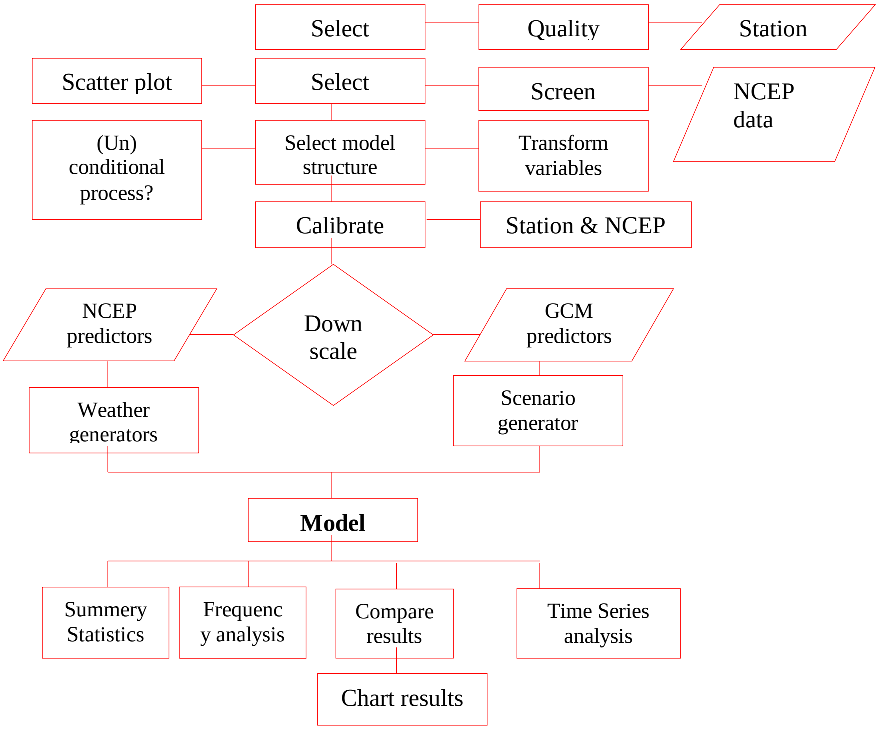

Figure 2 Schematic process of SDSM [63].

3 Result and Discussion

3.1 Trend Analysis

The nonparametric MK trend analysis for observed seasonal and annual precipitation data was tested at α = 0.05 (95%) significant level. The trend analysis was carried out on a seasonal basis by dividing the whole year into three seasons based on wet months. The first, second and third season are March to May, June to August and September to October respectively. Precipitation was trendless in season two at all stations. An increasing trend was observed during season one at Hagere Selam station and Arba Minch, Bilate, Hagere Mariam and Mirab Abaya stations during season three.

The annual trend test result shows an increasing trend at Hagere Selam and Mirab Abaya stations. This classification was based on the rainfall trend in the sub-basin. Table 2 summarizes the significance level of the seasonal rainfall trend analysis for each station during the study period 1988-2015.

Table 2 Seasonal and annual MK trend test.

Station	S_1		S_2		S_3		Annual	
	Mean	**Z**	**Mean**	**Z**	**Mean**	**Z**	**Mean**	**Z**
Alaba Kulito	337.4	-0.968	367.0	0.000	251.6	0.059	1057.4	-1.403
Arba Minch	366.8	0.553	158.5	0.336	221.7	**2.233**	928.5	1.205
Bilate	280.3	0.731	253.3	0.375	200.7	**2.470**	822.5	0.533
Boditi	412.2	-0.375	434.4	-0.612	260.6	1.087	1220.3	-1.047
Chencha	451.3	-0.257	321.0	-1.758	373.9	0.612	1284.3	-0.968
Dilla	539.1	0.474	332.5	0.059	440.1	1.600	1447.2	0.178
Fiseha Genet	494.4	1.047	278.6	-0.336	462.8	1.719	1367.5	0.454
Hagere Mariam	414.4	-0.415	150.9	0.652	268.4	**2.233**	898.0	1.324
Hagere Selam	451.0	**2.154**	379.4	0.237	371.5	1.600	1317.5	**2.074**
Haisawita	399.0	0.375	320.5	0.375	289.9	1.442	1109.8	0.533
Hawassa	294.3	0.968	347.5	1.166	221.6	-0.257	956.4	0.138
Hossana	375.4	0.000	462.6	0.573	244.8	-0.178	1178.7	-0.751
Mirab Abaya	297.0	0.968	191.0	1.363	223.6	**2.628**	793.7	**2.746**
Yirga Chefe	552.4	0.099	307.1	1.008	414.0	0.296	1365.9	0.652

S-season, Z-MK test statistics: bold marks indicate significant values at $\alpha = 0.05$ significance level.

3.2 Drought Events

The 3-month SPI gives a correlation of the precipitation over a particular 3-month time span with the total precipitation from a similar 3-month term for every one of the years included in the historical record and the future scenario data. In essentially agricultural districts, a 3-month SPI may be more successful in determining accessible moisture conditions than the moderate reacting Palmer Index or other accessible hydrological indices [59].

A 12-month SPI is a correlation between the precipitation in 12 back-to-back very long time periods and that recorded in 12 successive months in every prior year of accessible data. Since these timescales are aggregated after shorter periods that may be above or below normal, most SPIs have a tendency to incline toward zero unless an unmistakable wet or dry pattern is occurring. It is imperative to use both the 3-month SPI and a longer timescale (12-month SPI) [59]. The 3-month and 12-month SPIs were computed using both observed precipitation data from 1988 to 2015 and simulated precipitation data based on RCP scenarios from 2016 to 2100 simultaneously.

Based on the record historical precipitation, 3-month and 12-month SPI analysis indicated SPI < 0, i.e. drought occurred for more than fifty percent of the sub-basin area in the years 1990-1991, 1994, 1997, 1999-2000, 2002, 2004, 2008, 2011-2012 and 2015. During drought periods, the average annual precipitation in the sub-basin was between 77 mm to 84 mm, an amount that is below normal (average). In 2000, except for the Chencha and Yirga Chefe stations, extreme drought occurred at all stations in the 3-month SPI for the month of March (Figure 4). Generally, in the sub-basin, the drought frequency is three years due to the impact of Indian Ocean Dipole (IOD), a La Niña episode or an El Niño episode [68,69]. Plots of the time series of 3-month and 12-month SPI outputs at Arba Minch and Dilla stations are shown in Figure 3.

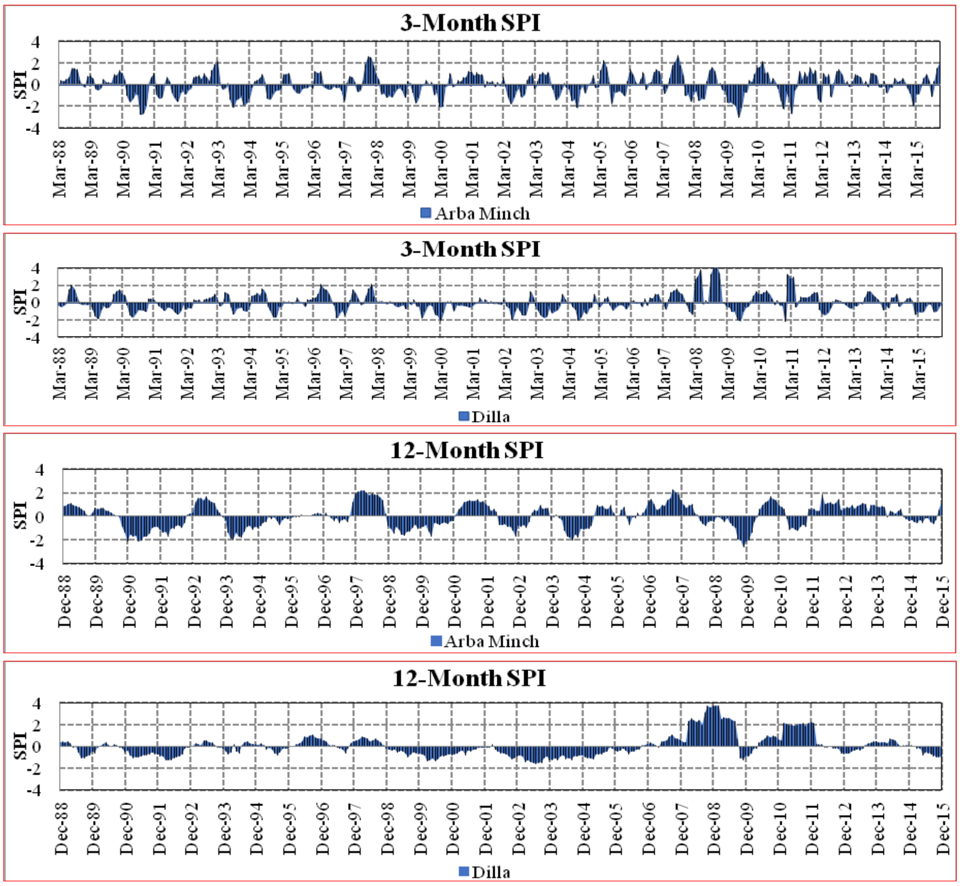

Figure 3 3-month and 12-month SPIs at Arba Minch and Dilla stations.

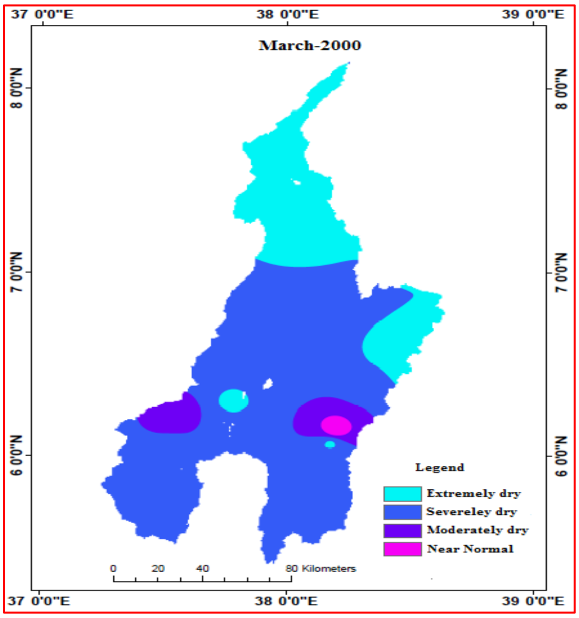

Figure 4 Spatial distribution of drought events in March 2000.

Drought in the sub-basin was analyzed for each time scale based on the rare event of every occasion for each station regarding the total number of perceptions over the sub-basin in the same event and time scale. The lowest annual rainfall was recorded in Mirab Abaya station; this area was more affected by drought than the others. Table 3 shows the percentage of drought events at 3- and 12-month time scales in the sub-basin. Near-normal drought is indicated by the highest percentage of drought events occurring in the sub-basin and extreme drought is indicated by the lowest percentage.

Future precipitation data were simulated using a GCM considering RCP scenarios. Relative to the reference period 1988 to 2015, the predicted SPI result shows an increasing drought frequency. 3-SPI below -1.0 was 15.6%, 21.7%, 20.1% and 19.8 % in 1988 to 2015, 2016 to 2040, 2050s and 2080s respectively. 12-SPI below -1.0 was 15.2%, 20.6%, 18.9% and 18.8 % in 1988 to 2015, 2016 to 2040, 2050s and 2080s respectively.

The predicted SPI analysis indicates increasing drought events in all scenarios relative to the reference period. Drought event conditions can be provoked by changes in precipitation and other climatic variables because of climate change [70]. Therefore, future drought events in the study area are strongly affected by climate change.

Table 3 Percentage of drought occurrence in the Abaya Chamo Sub-basin .

Drought Event	3-SPI				12-SPI			
	1988 to 2015	2016 to 2040	2050s	2080s	1988 to 2015	2016 to 2040	2050s	2080s
Extremely dry	2.3	4.8	4.6	4.9	1.6	3.6	3.1	3.1
Severely dry	4.2	6.0	5.0	5.1	3.5	4.3	4.4	4.9
Moderately dry	9.1	10.8	10.5	9.7	10.1	12.7	11.4	10.9
Near-normal	68.9	60.7	77.3	64.5	69.0	62.6	76.4	69.8

3.3 SDSM Result

3.3.1 Model Calibration and Validation

The selected appropriate NECP-NCAR predictors and daily precipitation predictands were used for model calibration and validation. The data from 1988 to 2003 and 2004 to 2015 were used for model calibration and validation respectively. For precipitation, a conditional process was selected and an event threshold of 0.3 mm/day [63] was used. The weather generator model enables the confirmation of the calibrated model and can be used to reconstruct predictands [63].

Table 4 Statistical evaluation of model performance.

Stations	Calibration			Validation		
	R^2	NSE	PBIAS	R^2	NSE	PBIAS
Alaba Kulito	0.78	0.72	9.1	0.9	0.53	7.1
Arba Minch	0.67	0.5	23.1	0.82	0.74	14.8
Bilate	0.92	0.6	17.9	0.92	0.85	10.9
Boditi	0.96	0.91	9.3	0.96	0.85	16
Chencha	0.85	0.68	5.8	0.86	0.72	15.3
Dilla	0.84	0.65	23.9	0.62	0.56	4.9
Fiseha Genet	0.89	0.60	21.9	0.9	0.82	13.6
Hagere Mariam	0.79	0.58	24.2	0.94	0.76	24.1
Hagere Selam	0.89	0.65	16.4	0.97	0.95	6.1
Haisawita	0.69	0.56	10.1	0.81	0.77	2.5
Hawassa	0.87	0.59	16.4	0.97	0.66	21.8
Hossana	0.79	0.65	5.2	0.94	0.87	11.2
Mirab Abaya	0.91	0.62	17.5	0.87	0.60	13.8
Yirga Chefe	0.89	0.8	15.5	0.93	0.88	13.5

The output of the model was evaluated by coefficient of determination (R^2), Nash-Sutcliffe efficiency (NSE) and percent bias (PBIAS). In general, model simulation is evaluated as satisfactory if $R^2 > 5.0$, NSE > 5.0 and PBIAS ± 25%. The result in Table 4 shows that the model's performance was acceptable. Table 4 shows the performance of the model during calibration and validation. According to the result, the precipitation data produced by SDSM closely matched the observed precipitation during the calibration and validation period.

Figure 5 shows the observed and downscaled monthly precipitation data for a sample of the stations (Boditi, Chencha, Hawassa and Mirab Abaya) for the calibration and validation period.

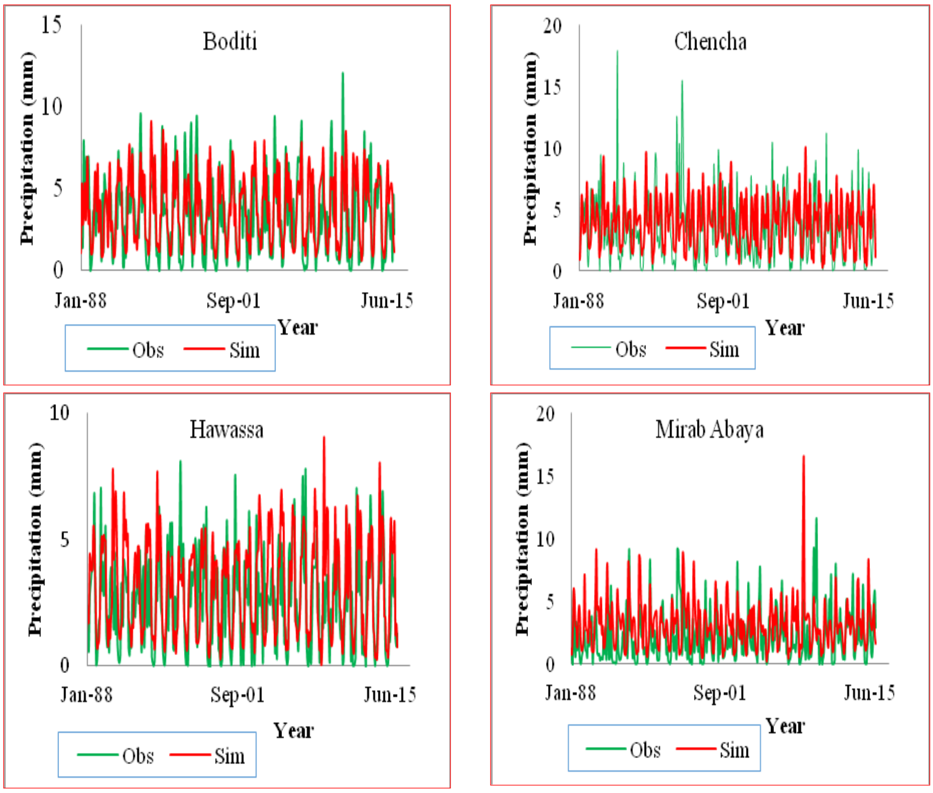

Figure 5 Observed and downscaled precipitation.

3.3.2 Projection of Future Precipitation Scenario

Future scenarios of daily precipitation were generated based on the predictors of several Can ESM2 models (RCP-2.6, -4.5 and -8.5) for the period of 2006 to 2100. To analyze the change in precipitation with reference to the observed precipitation data (1988-2015), three future climate windows were selected, i.e., 2016 to 2040, 2050s and 2080s.

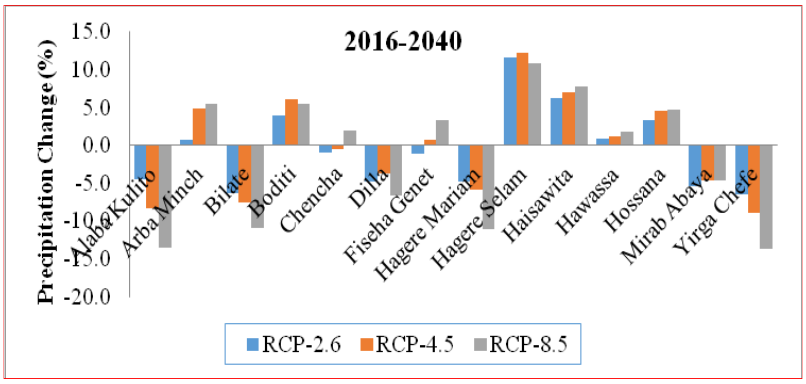

(a)

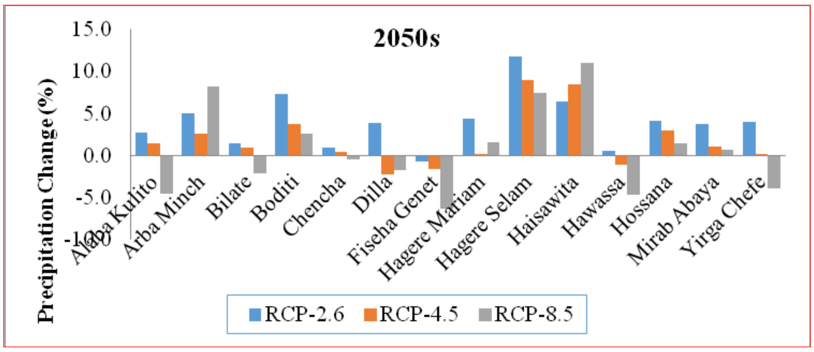

(b)

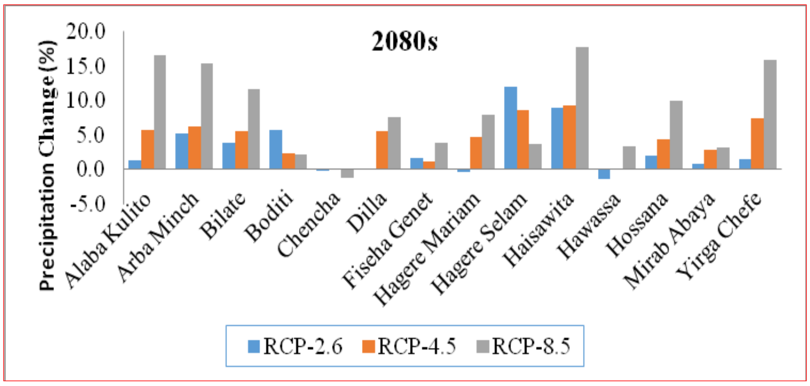

(c)

Figure 6 Precipitation scenarios change: (a) 2016-2040, (b) 2050s. (c) 2080s.

The average of the downscaled precipitation scenario decreases in the sub-basin for the future period of 2016 to 2040 and increases in the 2050s and 2080s. The decrease in mean annual precipitation varies from 0.9% to 6.5%, 0.2% to 8.9% and 1.4% to 13.7% for the stated time windows. The expected increase in mean precipitation varies from 0.5% to 11.7%, 0.2% to 8.9% and 0.6% to 11.1% for the 2050s period and 0.2% to 12.0%, 0.1% to 9.4% and 2.2% 17.8% for the 2080s period under all scenarios, respectively. This increase in precipitation may be attributed to an increase in surface temperature, which would raise the rate of evaporation, prompting increased precipitation [67] and a decrease in the impact of (IOD), La Niña episodes or El Niño episodes [68, 69]. Figure 6 shows the percentage of precipitation change expected for each station.

4 Conclusion

Drought events in the Abaya Chamo sub-basin in Ethiopia were estimated using the SPI method from observed precipitation data collected from fourteen meteorological stations for the period of 1988 to 2015. The analysis result indicates that for the 3-month and 12-month SPIs more than fifty percent of the sub-basin area is affected by moderate, severe and extreme droughts in 1990-1991, 1994, 1997, 1999-2000, 2002, 2004, 2008, 2011-2012 and 2015.

The average annual precipitation in drought periods was between 77 mm to 84 mm, which is below normal conditions. When precipitation is absent or below average, drought episodes are induced in the sub-basin. Droughts are due to the impact of IOD, La Niña or El Niño episodes. Such drought events in the sub-basin lead to harvest, failure, dwindling household income of rural communities and food insecurity. Observed and future precipitation can be used as appropriate input to study drought implications and probable consequences.

The future precipitation outputs obtained from a statistical downscaling model were subjected to trend analysis. The mean annual precipitation decreases by 0.2% to 13.7%, 0.5% to 6.4% and 0.1% to 1.3% for the period from 2016 to 2040, 2050s and 2080s respectively and the expected increase in mean precipitation varies from 0.5% to 11.7%, 0.2% to 8.9% and 0.6% to 11.1% in 2050s and 0.2% to 12.0%, 0.1% to 9.4% and 2.2% 17.8% in 2080s under the RCP-2.6, RCP-4.5 and RCP-8.5 scenarios respectively.

Despite the inherent uncertainties associated with the CanESM2 and SDSM models, it can be concluded that SDSM and SPI performed well on the Abaya Chamo sub-basin in downscaling future precipitation scenarios and for analysis of drought events.

Acknowledgements

The authors thankfully acknowledge the Ministry of Water, Irrigation and Energy, National Meteorological Agency, South National Nationalist People's Region Meteorological Agency, Ethiopia and the Canadian Center for Climate Modeling for providing the necessary data for this study, Arba Minch University for the financial support, the National Drought Mitigation Center, University of Nebraska-Lincoln for providing the SPI program and Dr. Wilby and Dawson for providing SDSM 4.2.

References

[1] Mishra, K.A. & Singh, V., *Drought Modeling: A Review*, J.Hydrol., **403**(1-2), pp. 157-175, 2011.

[2] Zarch, M.A.A., Sivakumar, B. & Sharma, A., *Droughts in a Warming Climate: A Global Assessment of Standardized Precipitation Index (SPI) and Reconnaissance Drought Index (RDI)*, J.Hydrol., **526**, pp. 183-195, 2015.

[3] Tabari, H., Abghari, H. & Talaee, P.H., *Temporal Trends and Spatial Characteristics of Drought and Rainfall in Arid and Semi-arid Regions of Iran*, Hydrol.Processes, **26**, pp. 3351-3361, 2012.

[4] Bayissa, Y.A., Moges, S.A., Xuan, Y., Andel, S.J.V., Maskey S., Solomatine, D.P., Griensven, A.V. & Tadesse, T., *Spatiotemporal Assessment of Meteorological Drought under the Influence of Varying Record Length: The Case of Upper Blue Nile Basin, Ethiopia*, Hydrological Sciences Journal, **60**, pp. 1927-1942, 2015.

[5] Bordi, I., Fraedrich, K. & Sutera, A., *Observed Drought and Wetness Trends in Europe: an Update*, Hydrol. Earth Syst. Sci., **13**, pp. 1519-1530, 2009.

[6] Minetti, J.L., Vargas W.M., Poblete A.G., Zerda L.R.d.l. & Acuña L.R., *Regional Droughts in Southern South America*, Theor. Appl. Climatol, **102**(3-4), pp. 403-415, 2010.

[7] Feng, S., Hu, Q. & Oglesby, R.J., *Influence Of Atlantic Sea Surface Temperatures on Persistent Drought in North America*, Clim. Dyn, **37**(3-4), pp. 569-586, 2011.

[8] Hannaford, J., Lloyd-Hughes, B., Keef, C., Parry, S. & Prudhomme, C., *Examining the Large-scale Spatial Coherence of European Drought Using Regional Indicators of Precipitation and Streamflow Deficit*, Hydrol. Process, **25**, pp. 1146-1162, 2011.

[9] Fang, K., Gou, X., Chen, F., Davi, N. & Liu, C., *Spatiotemporal Drought Variability for Central And Eastern Asia over the Past Seven Centuries Derived from Tree-Ring Based Reconstructions*, Quat. Int., **283**, pp. 107-116, 2013.

[10] Hua, T., Wang X., Zhang, C. & Lang, L., *Temporal and Spatial Variations in the Palmer Drought Severity Index over the Past Four Centuries in Arid, Semiarid, and Semihumid East Asia*, Chin. Sci. Bull., **58**(33), pp. 4143-4152, 2013.

[11] Buttafuoco, G., Caloiero, T. & Coscarelli, R., *Analyses of Drought Events in Calabria (southern Italy) Using Standardized Precipitation Index Water*, Resour. Manag., **29**(2), pp. 557–573, 2015.

[12] Sirangelo, B., Caloiero T., Coscarelli, R. & Ferrari, E., *Stochastic Analysis of Long Dry Spells in Calabria (Southern Italy)*, Theor. Appl. Climatol, **127**(3-4), pp. 711–724, 2017.

[13] Tsakiris, G., Pangalou, D. & Vangelis, H., *Regional Drought Assessment Based on the Reconnaissance Drought Index (RDI)*, Water Resources Management, **21**(5), pp. 821-833, 2007.

[14] Caloiero, T., *Drought Analysis in New Zealand Using the Standardized Precipitation Index*, Environ. Earth Sci, **76**, p. 569, 2017.

[15] Capra, A. & Scicolone, B., *Spatiotemporal Variability of Drought on a Short-Medium Time Scale in the Calabria Region (Southern Italy)*, Theor. Appl. Climatol, **100**(3), pp. 471-488, 2012.

[16] Wu, H., Hayes, M.J., Wilhite, D.A. & Svoboda, M.D., *The Effect in the Length of Record in the Standardized Precipitation Index Calculation*, Int. J. Climatol, **25**(4), pp. 505-520, 2005.

[17] Vicente-Serrano, S., *Differences in Spatial Patterns of Drought on Different Time Sales, An Analysis of the Iberian Peninsula*, Water Resources Management, **20**(1), pp. 37-60, 2006.

[18] Caloiero, T., Sirangelo, B., Coscarelli, R. & Ferrari, E., *An Analysis of the Occurrence Probabilities of Wet and Dry Periods through a Stochastic Monthly Rainfall Model*, Water, **8**(2), p. 39, 2016.

[19] Stephanie, G., Noel, K., Ellen, V. & Diriba, K., *The El Nino Effect on Ethiopian Summer Rainfall*, Climate Dynamics, 49(5-6), pp. 1865-1883, 2017.

[20] Library of Congress, *Ethiopia, A Country Study Handbook*, Library of Congress, http://countrystudies.us/ethiopia/41.htm, (January 8 2018).

[21] Cheung, W., Senay, G. & Singh, A., *Trends and Spatial Distribution of Annual and Seasonal Rainfall in Ethiopia*, International Journal of Climatology, **28**, pp. 1723-1734, 2008.

[22] Ethiopian Treasures, *Climate: Ethiopian Seasons*, www.ethiopiantreasures.co.uk/pages/climate.htm, (January 27 2018).

[23] Gleixner, S., Keenlyside, N., Viste, E. & Korecha, D., *The El Niño Effect on Ethiopian Summer Rainfall*, Climate Dynamics, **49**, pp. 1865-1883, 2017.

[24] Seleshi, Y. & Zanke U., *Recent Changes in Rainfall And Rainy Days in Ethiopia*, International Journal of Climatology, **24**, pp. 973-983, 2004.

[25] Edossa, D.C., Babel M.S. & Gupta A.D., *Drought Analysis in the Awash River Basin, Ethiopia*, Water Resources Management, **24**, pp. 1441-1460, 2010.
[26] Workineh, D., *Some Aspects of Meteorological Drought in Ethiopia. In Drought and Hunger in Africa: Denying Famine a Future*, Illustrated, Reprint, Revised Ed., Cambridge University Press, 1987.
[27] Hurni, H., *Land Degradation, Famine, and Land Resources Scenarios in Ethiopia*, Cambridge University Press, 1993.
[28] Dejene, A. & Yilma S., *Causes and Variability of Ethiopian Agriculture: Modeling the Relative Importance of Environment Factors, External Shocks, and State Policies 1980-1997*, in First International Policy Research Workshop in Regional and Local Development Studies on Environmental Management and Local Development in the Horn and East Africa (Bekure W. Semait Ed.), Regional and Local Development Studies (RLDS), Addis Ababa University, Addis Ababa, Ethiopia, pp. 17-54, 2003.
[29] Camberlin, P., *Rainfall Anomalies in the Source Region of the Nile and Their Connection with the Indian Summer Monsoon*, Journal of Climate, **10**, pp. 1380-1392, 1996.
[30] USAID, *El Niño in Ethiopia: Uncertainties, Impacts and Decision-making*, Feinstein International Center, Friedman School of Nutrition Science and Policy, Tufts University, 2015.
[31] Tiruneh, A.T., *Water Quality Monitoring in Lake Abaya and Lake Chamo Region*, PhD thesis, Chemistry-Biology, University of Siegen, Siegen, 2005.
[32] Awulachew, S.B., *Abaya-Chamo Lakes Physical and Water Resources Characteristics, including Scenarios and Impacts*, in Lake Abaya-Chamo Research Symposium, Arba Minch University, Arba Minch, 2007.
[33] Canada, C.C.f.C.M.a.A.o.E.a.C.C., *CanESM2 Predictors: CMIP5 experiments, Government of Canada*, http://climate-scenarios.canada.ca/?page=pred-canesm2, (10 January 2018).
[34] Subramanya, K., *Engineering Hydrology*, Tata McGraw-Hill Publishing Company Limited, 1994.
[35] Searcy, J. & Hardison, C., *Double-mass Curves: Manual of Hydrology-Part 1. General Surface-Water Techniques*, United-States Government Printing Office, 1960.
[36] Ahmad, I., Tang, D., Wang, T., Wang, M. & Wagan, B., *Precipitation Trends over Time Using Mann-Kendall and Spearman's rho Tests in Swat River Basin, Pakistan*, Advances in Meteorology, **2015**, pp. 1-15, 2015.
[37] Jhajharia, D. & Singh, V., *Trends in Temperature, Diurnal Temperature Range and Sunshine Duration in Northeast India*, International Journal of Climatology, **31**, pp. 1353-1367, 2011.

[38] Dinpashoh, Y., Jhajharia, D., Fakheri-Fard, A., Singh, V. & Kahya, E., *Trends in Reference Crop Evapotranspiration over Iran*, Journal of Hydrology, **399**, pp. 422-433, 2011.

[39] Wagesho, N., Goel, N. & Jain, M., *Investigation of Non-stationarity in Hydro-climatic Variables at Rift Valley Lakes Basin of Ethiopia*, Journal of Hydrology, pp. 113-133, 2012.

[40] Douglas, E., Vogel, R. & Kroll, C., *Trends in Floods and Low Flows in the United States: Impact of Spatial Correlation*, Journal of Hydrology, **240**, pp. 90-105, 2000.

[41] Kahya, E. & Kalayci, S., *Trend Analysis of Streamflow in Turkey*, Journal of Hydrology, **289**, pp. 128-144, 2004.

[42] Xu, Z., Takeuchi, K. & Ishidaira, H., *Monotonic Trend and Step Changes in Japanese Precipitation*, Journal of Hydrology, 279, pp. 144-150, 2003.

[43] Partal, T. & Kahya, E., *Trend Analysis in Turkish Precipitation Data*, Hydrology Processes, **20**, pp. 2011-2026, 2006.

[44] Jhajharia, D., Shrivastava, S., Sarkar, D. & Sarkar, S., *Temporal Characteristics of Pan Evaporation Trends under the Humid Conditions of Northeast India*, Agricultural and Forest Meteorology, **149**, pp. 763-770, 2009.

[45] Tebakari, T., Yoshitani, J. & Suvanpimol, C., *Time-space Trend Analysis in Pan Evaporation over Kingdom of Thailand*, Journal of Hydrologic Engineering, **10**(3), pp. 205-215, 2005.

[46] Singh, P., Kumar, V., Thomas, T. & Arora, M., *Basin-wide Assessment of Temperature Trends in Northwest and Central India*, Hydrological Sciences Journal, **53**(2), pp. 421-433, 2008.

[47] Ayele, E. G., Chunju, Z., Yihong, Z. & Yang, Z., *Assessment of Future Temperature Change Scenario by Statistical Downscaling Model (CanESM2) in Abaya Chamo Sub-basin, Ethiopia*, International Journal of Current Research, **11**(1), pp. 100-109, 2019.

[48] Singh, P., Kumar, V., Thomas, T. & Arora, M., *Basin-wide Assessment of Temperature Trends in Northwest and Central India*, Hydrol.Sci.J., **53**, pp. 421-433, 2008.

[49] Keyantash, J. & Dracup, J., *An Aggregate Drought Index: Assessing Drought Severity Based on Fluctuations in the Hydrologic Cycle and Surface Water Storage*, Water Resources Research, **40**(9), W094304, 2004.

[50] Pandey, R., Mishra S., Singh, R. & Ramasastri, K., *Streamflow Drought Severity Analysis of Betwa River System (India)*, Water Resources Management, **22**(8), pp. 1127-1141, 2008.

[51] Palmer, W., *Meteorological Drought*, Research Paper, Office of Climatology, U.S. Weather Bureau, Washington, D.C., 1965.

[52] Stahl, K., *Hydrological Drought: A Study Across Europe*, Doctoral Dissertation, Geowissenschaftlichen Fakultät, Albert-Ludwigs Universität Freiburg, Freiburg, Germany, 2001.
[53] Fleig, A., Tallaksen, L., Hisdal, H., Stahl, K. & Hannah, D., *Intercomparison of Weather and Circulation Type Classifications for Hydrological Drought Development*, Physics and Chemistry of the Earth, **35**(9-12), pp. 507-515, 2010.
[54] Sharma, T. & Panu, U., *Analytical Procedures for Weekly Hydrological Droughts: a Case of Canadian rivers*, Hydrological Sciences Journal, **55**(1), pp. 79-92, 2010.
[55] McKee, T., Doesken, N. & Kleist, J., *The Relationship of Drought Frequency and Duration to Time Scales*, In Eighth Conference on Applied Climatology, Anaheim, California, USA, pp. 179-184, 1993.
[56] Shukla, S. & Wood, A., *Use of a Standardized Runoff Index for Characterizing Hydrologic Drought*, Geophysical Research Letters, **35**, p. L02405, 2008.
[57] Akbari, H., Rakhshandehroo, G., Sharifloo, A. & Ostadzadeh, E., *Drought Analysis Based on Standardized Precipitation Index (SPI) and Streamflow Drought Index (SDI) in Chenar Rahdar River Basin, Southern Iran*, Watershed Management, pp. 11-22, 2015.
[58] Nalbantis, I., *Evaluation of a Hydrological Drought Index*, European Water, **23/24**, pp. 67-77, 2008.
[59] World Meteorological Organization, *Standardized Precipitation Index: User Guide*, World Meteorological Organization (WMO), 2012.
[60] Guenang, G. & Kamga, F., *Computation of the Standardized Precipitation Index (SPI) and Its Use to Assess Drought Occurrences in Cameroon over Recent Decades*, Journal of Applied Meteorology and Climatology, **53**, pp. 2310-2324, 2014.
[61] Guttman, N., *Comparing the Palmer Drought Index and the Standard Precipitation Index*, Journal of the American Water Resources Association, **34**(1), pp. 113-121, 1998.
[62] Juliani, B.H.T. & Okawa, C.M.P., *Application of a Standardized Precipitation Index for Meteorological Drought Analysis of the Semi-Arid Climate Influence in Minas Gerais, Brazil*, Hydrology, **4**(2), Article No. 26, 2017. DOI: 10.3390/hydrology4020026.
[63] Wilby, R., Dawson, C. & Barrow, E., *SDSM-A Decision Support Tool for the Assessment of Regional Climate Change Impacts*, Environmental Modelling & Software, **17**, pp. 147-159, 2002.
[64] Wilby, R. & Dawson, C., *Statistical Downscaling Model (SDSM)*, Version 4.2, Department of Geography, Lancaster University, UK, 2007.
[65] Hewitson, B. & Crane, R. G., *Climate Downscaling: Techniques and Application*, Climate Journal, **7**, pp. 85-95, 1996.

[66] Singh, D., Jain S. & Gupta R., *Statistical Downscaling and Projection of Future Temperature and Precipitation Change in Middle Catchment of Sutlej River Basin, India*, Jounal of Earth System, **124**, pp. 843-860, 2015.

[67] Anandhi, A., Srinivas, V.V., Kumar, D.N. & Nanjundiah, R.S., *Role of Predictors in Downscaling Surface Temperature to River Basin in India for IPCC SRES Scenarios Using Support Vector Machine*, International Journal of Climatology, **29**, pp. 583-603, 2009.

[68] FAO, *FAO Ethiopia Drought Response Plan and Priorities in 2017,* Revised version, August 2017, FAO, https://reliefweb.int/report/ethiopia/fao-ethiopia-drought-response-plan-and-priorities-2017-revised-version-august-2017, (January 25 2018).

[69] WFP, *Joint Government and Humanitarian Partners' Revised Humanitarian Requirements Document for South and Southeastern Parts of the Country*, WFP, http://vam.wfp.org/CountryPage_assessments.aspx?iso3=ETH, (January 25 2018).

[70] Lee, S-H., Yoo, S-H., Choi J-Y. & Bae, S., *Assessment of the Impact of Climate Change on Drought Characteristics in the Hwanghae Plain*, North Korea Using Time Series SPI and SPEI: 1981-2100, Water, **9**(579), pp. 1-19, 2017.